



# Polarization-dependent C K near-edge X-ray absorption fine-structure of graphene

M. Papagno<sup>a,\*</sup>, A. Fraile Rodríguez<sup>b</sup>, Ç.Ö. Girit<sup>c,d</sup>, J.C. Meyer<sup>c,d</sup>, A. Zettl<sup>c,d</sup>, D. Pacilé<sup>a</sup>

<sup>a</sup> Istituito Nazionale di Fisica Nucleare (INFN) and Dip. di Fisica Università della Calabria, 87036 Arcavacata di Rende, Cosenza, Italy

<sup>b</sup> Swiss Light Source, Paul Scherrer Institut, 5232 Villigen PSI, Switzerland

<sup>c</sup> Department of Physics, University of California, Berkeley, CA 94720, USA

<sup>d</sup> Materials Sciences Division, Lawrence Berkeley National Laboratory, Berkeley, CA 94720, USA

## ARTICLE INFO

### Article history:

Received 3 March 2009

In final form 22 May 2009

Available online 27 May 2009

## ABSTRACT

We report the polarization-dependent C K photoabsorption spectra of single- and few-layer graphene (FLG) samples produced by micromechanical cleavage of highly ordered pyrolytic graphite (HOPG) on a SiO<sub>2</sub> substrate. We show that the unoccupied  $\sigma$  density of states of graphene and FLG strongly reflects the one measured on bulk HOPG, demonstrating the two-dimensional character of  $\sigma$  states as well as the very-weak interlayer couplings between planes. Moreover, our spectra taken with different polarization allow us to show the predicted hybrid nature of the interlayer state.

© 2009 Elsevier B.V. All rights reserved.

## 1. Introduction

Graphene is an exciting new material with unusual properties that has several application potentials ranging from nanoelectronics to single molecule gas detectors [1,2]. It consists of a single atomic layer of carbon atoms, and while it shares the same building block of graphite and carbon nanotubes, graphene has unique electronic properties. In particular, several exotic phenomena in single-layer graphene have been reported, such as integer quantum Hall effect [3], high carrier mobility [4], and long-range ballistic transport [5]. These properties are ascribable to the different behavior of electrons and holes respect to conventional semiconductors. Charge carriers in graphene can in fact be considered as massless Dirac fermions [6] with a constant speed ( $v_F$ ) that does not depend on their kinetic energy. Moreover, graphene electronic bands lack of an energy gap, having at most a vanishing density of states (DOS) at the Fermi energy, in correspondence to the K points of the Brillouin zone (BZ) [7] where the conduction and valence bands are degenerate.

In the present work, we have focused our attention on the symmetries of the lowest unoccupied electronic states of graphene. In graphene, the carbon atoms are assembled in a hexagonal lattice with two carbon atoms per unit cell. Since each carbon atom has four electrons available for bonding, three of them form strong covalent bonds with three neighboring atoms through  $sp^2$  orbitals and form  $\sigma$  states lying in the graphene (basal) plane. The fourth electron with  $p_z$  symmetry (perpendicular to the basal plane, namely along the  $c$ -axis) builds up the highest occupied valence band ( $\pi$ ) state. Both  $\sigma$  and  $\pi$  bands have their replica on the unoc-

cupied side of the DOS,  $\sigma^*$  and  $\pi^*$  states, respectively. The two-dimensional nature of graphene is therefore strongly reflected on the high-directionality of its orbitals, namely parallel to the basal plane or perpendicular to it. By using the near-edge X-ray absorption fine-structure (NEXAFS) technique it is therefore possible to excite electrons from the initial K-shell state into  $\pi^*$  or  $\sigma^*$  final states, depending on the orientation of the incident photon polarization vector with respect to the basal plane.

In our previous study [8] we reported the C K edge NEXAFS spectra of single and few-layer graphene (FLG) measured by photoemission electron microscopy (PEEM), with the photon linear polarization vector almost perpendicular to the basal plane of graphene, for which transitions into final states of  $\pi$  symmetry are enhanced. Those spectra reflect peculiar properties of the unoccupied DOS of single-layer graphene, and its evolution with an increasing number of layers towards the electronic states of bulk graphite.

Here, we have performed polarization-dependent NEXAFS studies of single- and multi-layers graphene flakes, showing the symmetry of final states. Our measurements allow also to support the interpretation of the interlayer state of graphene as originating from states with mixed  $\sigma$  and  $\pi$  character.

## 2. Experimental

Graphene samples were obtained by micromechanical cleavage of highly oriented pyrolytic graphite (HOPG) on a SiO<sub>2</sub> substrate. Single- and multi-layers flakes were identified by means of optical microscopy (OM) and Raman spectroscopy measurements [9,10]. The laterally resolved NEXAFS experiments were performed at the Surface/Interface:Microscopy (SIM) beamline [11] of the Swiss Light Source, using an Elmitec PEEM equipped with an energy analyzer. Element-specific PEEM contrast was obtained by dividing

\* Corresponding author. Present address: Istituto di Struttura della Materia-Consiglio Nazionale delle Ricerche, Trieste, Basovizza (TS), Italy.

E-mail address: [marco.papagno@ism.cnr.it](mailto:marco.papagno@ism.cnr.it) (M. Papagno).

pairs of images recorded at the C K absorption edge (285.5 eV) and below the edge (282.2 eV), thus reducing topographic effects and enhancing the chemical contrast. NEXAFS measurements were obtained by processing stacks of PEEM images obtained by scanning the incident photon energy across the C K edge. The measured total electron yield (TEY) of the region of interest was then normalized to the TEY collected from an area of the substrate. Measurements were performed at grazing incidence ( $16^\circ$  respect to the basal plane) with the linear polarization vector nearly-parallel ( $\mathbf{E}_1$ ) or perpendicular ( $\mathbf{E}_2$ ) to the  $c$ -axis, as reported in Fig. 2.

### 3. Results and discussion

The OM and PEEM images of the sample under investigation are shown in Fig. 1. The thickness of the various layers was determined by means of the so-called OM contrast method [9]. The very strong elemental contrast of PEEM allows to clearly distinguish between single, bilayer and FLG flakes.

In Fig. 2, we show NEXAFS measurements recorded by using the photon polarization vector  $\mathbf{E}_2$  for single- and four-layers graphene. As can be seen, the corresponding spectra are nearly identical. In particular, the four-layers spectrum can be obtained by the single-layer spectrum multiplied by a factor of four, to take into account the four times higher number of absorbing atoms per unit area (dot curve in Fig. 2). This result was somehow expected as in this geometry we are mainly investigating the intra-layer unoccupied electronic states, which are, in the investigated energy

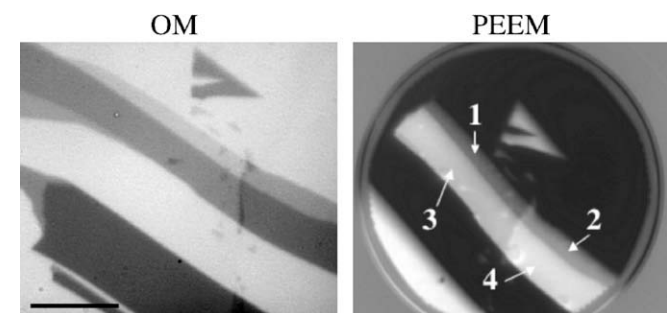


Fig. 1. OM (left) and PEEM (right) images of the investigated sample. Scale bar corresponds to  $10 \mu\text{m}$ . The number of layers is reported on the PEEM image.

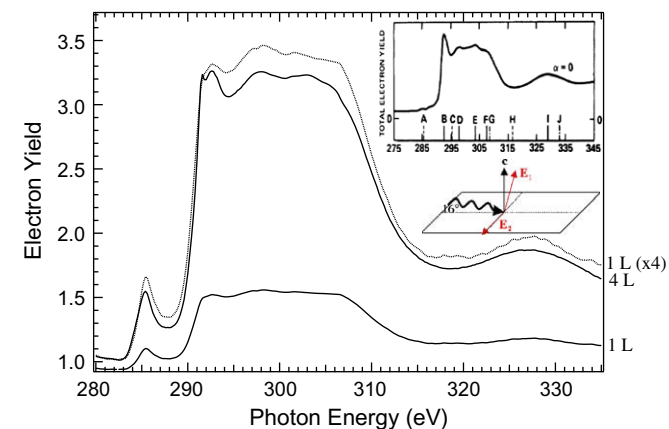


Fig. 2. C K edge photoabsorption spectra of single- and four-layers graphene flakes from sample of Fig. 1, recorded with polarization  $\mathbf{E}_2$ . The dot line represents the spectrum for single-layer multiplied by a factor of 4. The inset shows NEXAFS spectrum of HOPG measured at normal incidence. From Ref. [12]. The scattering geometry of our experiment along with the two used vector polarization are reported.

region, unaffected by interlayer interactions. To further support our finding we note that our data match perfectly with previous NEXAFS experiments performed on HOPG, showed as an inset of Fig. 2 [12]. The peaks assignment is then straightforwardly obtained by comparing the peak positions of Fig. 2 with the graphite band structure. In this view, the first peak that appears at about 286 eV in our spectra (A peak in the inset) corresponds to the  $\pi^*$  resonance, namely to the electronic transition from the C(1s) level to the conduction  $\pi^*$  states at M and L point of the BZ. This transition should be forbidden by selection rules in this geometry, however we see a residual intensity corresponding to an angle of about  $15^\circ$  between the polarization vector and the basal plane. We estimated this value by comparing the peak intensity ratio  $\pi^*/\sigma^*$  from our data with that of graphite [12]. We believe that this result is ascribable to the roughness of graphene on  $\text{SiO}_2$  [13,14]. Strong corrugations with an average lateral dimension of a few nanometers and a vertical one of few Angstroms have been found on graphene flakes, due to the roughness of the  $\text{SiO}_2$  substrates. These corrugations lead to a distortion of the basal plane with respect to the undistorted plane, thus resulting in a non-vanishing  $\pi^*$  peak in our NEXAFS spectra for  $\mathbf{E}_2$  polarization vector.

The main peak at about 292 eV (B peak) corresponds to the  $\sigma^*$  threshold. This peak is composed of two distinct features at 291.8 eV and 292.7 eV. The sharp feature at 291.8 eV reflects strong correlation effects of electron-hole pairs within the flake, whereas the broad peak at 292.7 eV is related to the transition from C(1s) state to  $\Gamma_6^-$  and  $\Gamma_5^+$  bands at Gamma point of the BZ [15]. The peak at 297.8 eV (D peak) is due to C(1s)  $\rightarrow \Gamma_3^+$  at the M point, while peaks at 302.6 and about 306 eV (E and F) to C(1s)  $\rightarrow \Gamma_3^+ + \Gamma_2^-$  around M and L points, and  $\Gamma_1^+ + \Gamma_4^-$  at M point, respectively. Finally, the extended X-ray absorption fine-structure (EXAFS) exhibits the characteristic higher energy hump at 327 eV, which encloses information on the bond length and coordination number of C atoms within the basal plane [16].

In Fig. 3a, we show NEXAFS spectra for two different polarization vectors as a function of the number of layers, in the photon energy range from 280 to 305 eV. It is observed that for both  $\mathbf{E}_1$  and  $\mathbf{E}_2$  the spectral line-shape does not significantly change for an increasing number of graphene layers. A systematic improvement of the signal to noise ratio of the spectra is observed towards thicker layers due to the increasing number of absorption atoms. It is interesting to note here the different behavior of the two main resonances as the vector polarization is changed. In particular, the features at 286 and 292 eV exhibit opposite polarization dependence: the  $\pi^*$  excitation have maximum intensity for  $\mathbf{E}_1$  and minimum for  $\mathbf{E}_2$ . On the other hand,  $\sigma^*$  final states are enhanced for  $\mathbf{E}_2$  and suppressed for  $\mathbf{E}_1$ . These results are the direct consequence of the dipole selection rules and of the highly-oriented graphene final states involved in the NEXAFS process. In fact, since the observed features are due to transitions that involve the same initial state but final states having different symmetries, dipole selection rules state that transition matrix elements for  $\pi^*$  excitations are maximum (minimum) for  $\mathbf{E}$  perpendicular (parallel) to the surface. The opposite is true for  $\sigma^*$  final state transitions. Our result showed in Fig. 3a is independent of the thickness of the flake, confirming the layered structure of graphite. We note that both the residual intensity of the  $\pi^*$  resonance at  $\mathbf{E}_2$ , and the reduced intensity variation of the two resonances when switching from one polarization to the other one can be ascribed to the roughness of graphene flakes on  $\text{SiO}_2$ , as discussed above.

In Fig. 3b, we show a blow-up of the single-layer graphene spectrum measured for  $\mathbf{E}_2$  vector polarization. The spectrum clearly shows the presence of two distinct peaks located above and below the  $\pi^*$  resonance, at about 284 and 288 eV, respectively. We recently ascribed the former (pre-edge) peak to the van-Hove singularity of the unoccupied  $\pi$  electronic states at the M point of the BZ

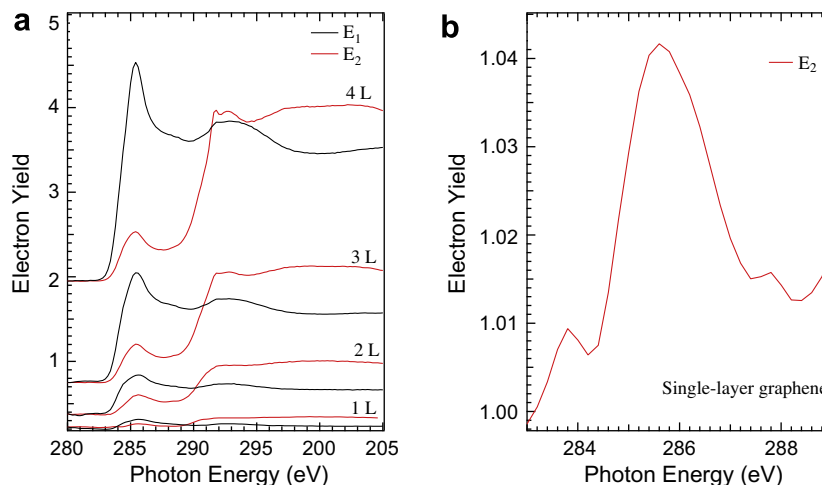


**Fig. 3.** (a) C K edge photoabsorption spectra from single- to four-layers graphene flakes measured with  $E_1$  (black curves) and  $E_2$  (red curves). (b) Zoom in of the single-layer graphene with  $E_2$  showing two additional peaks above and below the  $\pi^*$  main resonance. (For interpretation of the references to colour in this figure legend, the reader is referred to the web version of this article.)

[8]. We note that the reduced intensity of the  $\pi^*$  structure strongly favors the identification of the pre-edge peak. Theoretical and experimental works [17,18] have shown that both the pre-edge and the  $\pi^*$  resonance peaks split-up into two peaks as the number of layers is increased to two. This splitting should give rise to four peaks in our NEXAFS spectrum. Unfortunately, the limited energy resolution (about 0.2 eV) and the strongly enhanced intensity of the  $\pi^*$  peak do not allow us to resolve this double splitting. Nevertheless, our data show a pronounced increase of the full-width-half maximum (FWHM) of the  $\pi^*$  peak as we move from one (FWHM = 1.0 eV) to two-layers (FWHM = 1.4 eV), suggesting the occurrence of double peaks.

We now turn to the discussion of the second structure at about 288 eV. Based on previous NEXAFS data on HOPG [15] and on recent experiments and theoretical calculations [19], we ascribe this peak to the analog of the *interlayer state* of graphite. The discovery of this state in graphite has been of crucial importance to understand the physics of alkali intercalated compounds [15,20,21]. Interestingly, theoretical studies predict the existence of such state for single-layer systems also [22]. These results have been recently questioned [23] and the 288 eV structure has been ascribed to COOH and CH species related transitions, due to residual contaminants at the edges of HOPG flakes.

We have already showed [8,24] the presence of this peak when using  $E_1$  polarization vector. In Fig. 3b, we show that the 288 eV feature is clearly resolved for single-layer graphene and is also detectable as a shoulder in the two- and three-layers (not shown) with  $E_2$  polarization vector. We note that since the interlayer state is an antibonding state with mainly three-dimensional character it is expected to be mainly insensitive to the scattering geometry used in the experiment. We therefore believe that our latter finding further supports the interlayer state origin of the peak at 288 eV.

#### 4. Conclusions

We have performed polarization-dependent C K near-edge X-ray absorption fine-structure measurements of single- and multi-layers graphene samples produced by micromechanical cleavage of highly ordered pyrolytic graphite on  $\text{SiO}_2$  substrate. NEXAFS spectra show strong variations as the polarization is changed from parallel to normal respect to the surface, reflecting different final states symmetries involved in the absorption process. C K absorption spectra on single- and four-layers graphene recorded with

polarization vector within the basal plane match perfectly the ones measured on HOPG, confirming the same unoccupied  $\sigma$ -state-symmetry density of states for the two systems. Finally, our data allow to confirm the existence of the interlayer state for single- and multi-layers graphene.

#### Acknowledgements

Part of this work was performed at the Swiss Light Source, Paul Scherrer Institut, Switzerland. This research project has been supported by the European Commission under the 6th Framework Programme through the Key Action: Strengthening the European Research Area, Research Infrastructures. Contract No. R113-CT-2004-506008.

#### References

- [1] L.A. Ponomarenko, F. Schedin, M.I. Katsnelson, R. Yang, E.W. Hill, K.S. Novoselov, A.K. Geim, *Science* 320 (2008) 356.
- [2] F. Schedin, A.K. Geim, S.V. Morozov, E.W. Hill, P. Blake, M.I. Katsnelson, K.S. Novoselov, *Nature* 6 (2007) 652.
- [3] K.S. Novoselov et al., *Nature* 438 (2005) 197.
- [4] K.S. Novoselov et al., *Science* 306 (2004) 666.
- [5] C. Berger et al., *Science* 312 (2006) 1191.
- [6] A. Bostwick, T. Ohta, T. Seyller, K. Horn, E. Rotenberg, *Nature Phys.* 3 (2007) 36.
- [7] D.P. DiVincenzo, E.J. Mele, *Phys. Rev. B* 29 (1984) 1685.
- [8] D. Pacil  et al., *Phys. Rev. Lett.* 101 (2008) 066806.
- [9] Z.H. Ni et al., *Nano Lett.* 7 (2007) 2758.
- [10] A.C. Ferrari et al., *Phys. Rev. Lett.* 97 (2006) 187401.
- [11] C. Quitmann et al., *Surf. Sci.* 480 (2001) 173.
- [12] R.A. Rosenberg, P.J. Love, V. Rehn, *Phys. Rev. B* 33 (1986) 4034.
- [13] Y. Zhang et al., *Nature Phys.* 4 (2008) 627.
- [14] M. Ishigami, J.H. Chen, W.G. Cullen, M.S. Fuhrer, E.D. Williams, *Nano Lett.* 7 (2007) 1643.
- [15] D.A. Fischer, R.M. Wentzcovitch, R.G. Carr, A. Continenza, A.J. Freeman, *Phys. Rev. B* 44 (1991) 1427.
- [16] X. Weng, P. Rez, H. Ma, *Phys. Rev. B* 40 (1989) 4175.
- [17] S.B. Trickey, F. M ller-Plathe, G.H.F. Diercksen, J.C. Boettger, *Phys. Rev. B* 45 (1992) 4460.
- [18] T. Ohta, A. Bostwick, T. Seyller, K. Horn, E. Rotenberg, *Science* 313 (2006) 951.
- [19] V.N. Strocov, P. Blaha, H.I. Starnberg, M. Rohlfing, R. Claessen, J.-M. Debever, J.-M. Themlin, *Phys. Rev. B* 61 (2000) 4994.
- [20] Th. Fauster, F.J. Himpsel, J.E. Fischer, E.W. Plummer, *Phys. Rev. Lett.* 51 (1983) 430.
- [21] G. Cs nyi, P.B. Littlewood, A.H. Nevidomskyy, C.J. Pickard, B.D. Simons, *Nature Phys.* 1 (2005) 42.
- [22] M. Posternak, A. Baldereschi, A.J. Freeman, E. Wimmer, M. Weinert, *Phys. Rev. Lett.* 50 (1983) 761.
- [23] Hae-Kyung Jeong et al., *Phys. Rev. Lett.* 102 (2009) 099701, (Comment on [8]).
- [24] D. Pacil  et al., *Phys. Rev. Lett.* 102 (2009) 099702 (Reply to Comment).